Dynamical Heterogeneity in Glassy *o*-Terphenyl: Manifestation of Environment Changes in Photoisomerization Kinetics of Probe Molecules

S. Yu. Grebenkin* and B. V. Bol'shakov

Institute of Chemical Kinetics and Combustion, Novosibirsk 630090, Russian Federation

Received: December 15, 2006; In Final Form: March 5, 2007

A new method for the investigation of dynamical heterogeneity in glassy matrixes is presented and illustrated by the example of *o*-terphenyl (OTP). UV−vis absorption spectroscopy has been used to monitor the cis−trans isomerization kinetics of probe molecules in glassy OTP. The dependence of isomerization quantum yield on light intensity has been established. This dependence is shown to be due to the change in the local environment of the probe molecules. The simple model is suggested to estimate the time required for the environment to change, τ_{ex}. The τ_{ex} values from 2.6×10^2 to 1.9×10^5 s have been obtained for environments of molecules of 1-naphthylazomethoxybenzene (NAMB) in OTP over a temperature range from 244 to 204 K ($T_g + 1$ to $T_g - 39$ K). The temperature dependence of exchange time has a non-Arrhenius character. As the temperature decreases, an increase in exchange time slows down. The activation energy of the relaxation process is 54 kJ/mol over the range of 224−239 K.

1. Introduction

Behavior of a many glass-forming substances at temperatures near T_g gives evidence for regions of different molecular mobility, that is, for heterogeneity.[1−4] The dynamical properties of the regions can vary with time. In this case, the heterogeneity is said to be dynamical. The dynamical heterogeneity in glass-forming liquids and polymers was detected by NMR method,[5−7] dielectric relaxation,[8−11] by light scattering,[12,13] molecular probe rotations,[14−20] and some others.[21] As a rule, the studies were performed at temperatures above or near T_g.

On the other hand, it is known that the matrix heterogeneity manifests itself in the kinetics of elementary chemical reactions as a decrease in reagent reactivity during chemical process.[22] The isomerization reactions, being monomolecular, are of particular interest as a means for studying molecular dynamic in glassy matrixes. Indeed, the molecules residing in the domains of different dynamics have different rates of isomerization and can be used as probes for environments.

In solid matrixes, the isomerization of spiropyranes[23,24] and the cis−trans isomerization of stilbenes[25,26] and azo compounds[27−31] are studied most often. The interest in the latter is due also to employment of azo dyes in the devices designed to store information. The kinetics of these processes is, as a rule, nonexponential because of medium heterogeneity. The rate constant (or quantum yield) decreases during reaction.

Usually, in a glassy matrix, the time required for the environment to change (exchange time, τ_{ex}) exceeds the time of reaction τ_r. Therefore the reactivity of each molecule is constant during the reaction, and the kinetics can be described as a sum of individual exponential processes. If $\tau_r \gg \tau_{ex}$, then the distribution of molecules over reactivity is steady as the reaction proceeds. In this case, the kinetics obeys the normal law, which holds for liquids.

On the basis of this idea, the racemization kinetics of bridged paddled binaphthyls[32] and isomerization of merocyanine into the spiropyran[33,34] were used to study the reorganization of local environments in polymer matrixes. Isomerization kinetics in both cases (except the isomerization of smallest molecule[32]) are nonexponential, reflecting the segmental dynamics of the polymer matrix. The thermodynamic parameters for the matrix reorganization rate were calculated from the analysis of kinetic curves.[33]

Since the photoisomerization rate depends on light intensity, the τ_r/τ_{ex} ratio can be varied. At low light intensity, the isomerization time can exceed the lifetime of the local matrix structure ($\tau_r \gg \tau_{ex}$). In this case, a change in the local environment during irradiation will lead to the restoration of the initial distribution of the molecules over reactivity. At high light intensity ($\tau_r \ll \tau_{ex}$) the distribution will not be restored in the course of the reaction. A fraction of poorly reactive molecules will increase during the reaction. Thus, the kinetics of photoisomerization will differ for high and low light intensities. Comparing these kinetics, one can estimate the exchange time.

In the present work, we have investigated the kinetics of the cis−trans photoisomerization of azo compound 1-naphthylazomethoxybenzene in glassy *o*-terphenyl at various light intensities. The exchange times were measured at temperatures far below T_g for the first time.

2. Experimental

2.1. Experimental Setup. The isomerization kinetics were monitored by measuring sample absorbance (spectrophotometer Specord UV−vis, Carl Zeiss Jena) at the wavelength of an absorption maximum of the trans isomer (388 nm). The design of the spectrophotometer allows one to obtain absorbance values in digital form. The sketch of the experimental setup is depicted in Figure 1.

The temperature-controlled (temperature controller Polikon 613, Thermex, St. Petersburg) cell equipped with quartz windows was placed in the spectrophotometer. The cell was cooled by gaseous nitrogen.

* Corresponding author. E-mail: grebenk@ns.kinetics.nsc.ru.

10.1021/jp068619w CCC: $37.00
Published on Web 05/05/2007

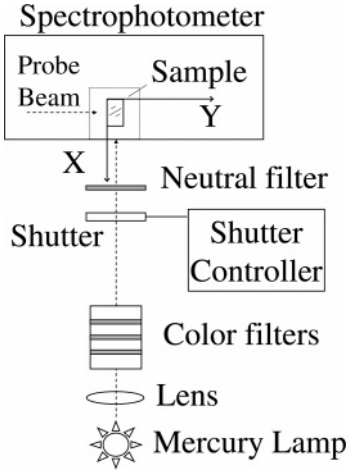

Figure 1. Schematic representation of the experimental setup.

Two different cells were used: aluminum and quartz. The design of the quartz cell allows one to turn the sample around the OZ axis. The sample temperature was kept constant to within ±0.2 K and ±0.1 K when employing quartz and aluminum cells, respectively. The measuring accuracy was ±0.5 K in any case. We used the quartz cell only when the turn of the sample was required. The aluminum one was employed in all other cases.

A 500 W high-pressure mercury arc lamp (DRSh-500-2M) operating on direct current was used as a source of irradiation light. The time stability of light flux was ±1% during the experiment. The photon flux at 546 nm measured by the rate of azobenzene photoisomerization in isooctane[35] was ~$(7.5 \pm 1.0) \times 10^{16}$ photon s^{-1} cm^{-2}. The light intensity at this photon flux was taken as 1 arbitrary unit (au). The required lines of the mercury spectrum were isolated using standard sets of colored glass filters immersed into the water bath. The light absorption by the sample at 546 nm did not exceed 1%; therefore, the light intensity was considered constant throughout the sample.

To obtain polarized light, the polarizers from LOMO PLC were used. We have experimentally determined that the contrast of the polarizer at 546 nm is more than 4.7×10^3. To polarize the probe beam, the polarizer was installed directly behind the probe light source inside the spectrophotometer. A homemade holder allows two fixed positions of the polarizer at which the probe light has either vertical or horizontal polarization. It takes less than 2 s to change the orientation of the polarizer. An incandescent lamp of 50 W (Royal Philips Electronics) was used as a probe light source.

To decrease the intensity of 546 nm light, the set of neutral glass filters NS7 and NS9 (transmittance of 0.0419), the filter NS8 (0.236), and the metal net (0.286) were used. The unattenuated light intensity is taken as 1 arbitrary unit.

2.2. Sample Preparation. The OTP powder (Fluka, ≥ 99.0% (GC), mp 329−332 K) was used as received. T_g for OTP determined by the calorimetric method is 243 K.[36]

1-naphthylazomethoxybenzene was synthesized in our laboratory in accordance with ref 37 and used after thin-layer chromatography purification. Its chemical structure is depicted in Figure 2.

Ampules of two types were used: a homemade Pyrex one with a rectangular cross section of 1 mm × 8 mm and a plastic one (Plastibrand, Brand) with a rectangular cross section of 4 mm × 10 mm. Correspondingly, the samples were prepared by the two following procedures.

In the first case, the ampule filled with the solution of NAMB in OTP (a concentration of 4×10^{-4} mol/L) was kept at 373−393 K for 2 h. On heating, the ampule was held at room temperature for 5 min and then irradiated with 405 nm light for 1 min to convert about 50% of NAMB into the cis form. In the second case, the Pyrex flask filled with the solution of NAMB in OTP (a concentration of 10^{-4} mol/L) was kept at 373−393 K for 2 h, then the solution was poured into the plastic ampule and irradiated with 405 nm light for 1 min at room temperature.

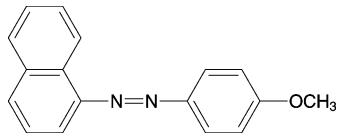

Figure 2. The chemical structure of NAMB.

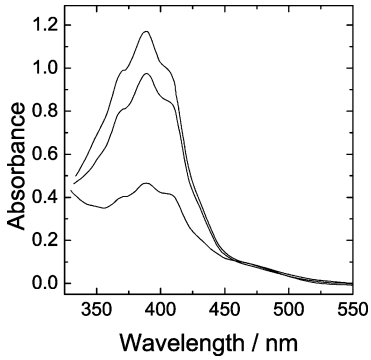

Figure 3. UV−vis absorption spectrums of NAMB in OTP. From top to bottom: before irradiation, after 2.5 h of irradiation with light of wavelength 546 nm, and after 0.5 h of irradiation with light of wavelength 405 nm, 239 K.

Following 405 nm irradiation, the ampule was housed in the cell and kept for 17 h at the experimental temperature. Thereafter, the kinetics of isomerization induced by 546 nm light was measured. We did not find a difference in kinetic curves obtained after 17 and 41 h (17 h + 24 h) of isothermal aging at 209, 229, and 239 K.

The samples did not crack and contained no bubbles. The plastic and Pyrex ampoules were irradiated in the directions parallel to the 10 and 8 mm edges, respectively. At each temperature, the kinetic curves were obtained using at least two light intensities.

2.3. Values under Measurement. Light-induced cis−trans isomerization of NAMB molecules in glassy OTP is accompanied by their orientation.[38] The time dependence of absorption is determined by both of the processes, and its interpretation is rather difficult. In order to obtain isomerization kinetics, that is, the time dependence of isomeric composition, we have recorded the absorption of the horizontally $Abs_\perp$ and vertically $Abs_\parallel$ polarized probe light at the same time. The combination of these values,

$$\mathrm{Abs}(t) = \frac{\mathrm{Abs}_\perp(t) + 2\mathrm{Abs}_\parallel(t)}{3} \qquad (1)$$

provides the value that is independent of angular particle distribution in our experimental conditions and directly proportional to the isomeric composition.

Figure 3 shows the optical absorption spectrums of NAMB in OTP before and after irradiation of the sample with light of wavelengths of 546 and 405 nm. The difference in the spectrums is caused by the different isomer ratios. Hereafter, absorbance denotes the value determined in accordance with eq 1.

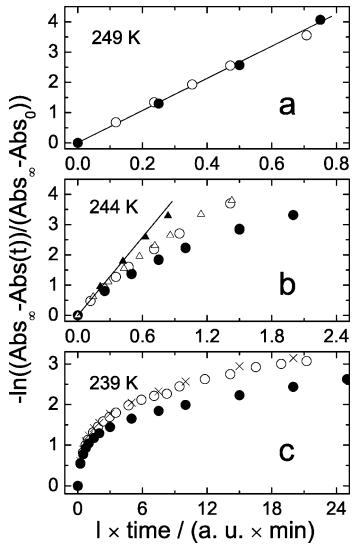

Figure 4. First-order plots for photoisomerization of NAMB in OTP at light intensity 1 (solid circles), 0.236 (open circles), 0.286 (open triangles), and 0.0419 a. u. (solid triangles). In addition, the kinetic curve obtained using the discontinuous irradiation with light of intensity 1 (the ratio of irradiation period to dark pause is equal to 1/3) is shown by crosses. Solid straight lines demonstrate an exponentiality of isomerization kinetics.

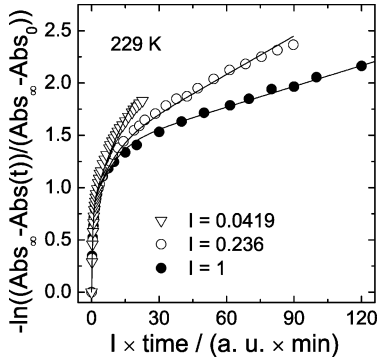

Figure 5. First-order plots for photoisomerization of NAMB in OTP at light intensity 1 (solid circles), 0.236 (open circles), and 0.0419 a.u. (triangles). Solid lines are results of fitting the data with the model described in the text.

The rate of dark cis → trans isomerization in the temperature range used in this work is quite negligible.

3. Results and Discussion

3.1. Dependence of Isomerization Quantum Yield on Light Intensity. At 249 K and higher, the kinetics of cis−trans isomerization obeys the exponential law, and the isomerization rate is proportional to light intensity. At 244 K and below, the shapes of kinetic curves depend on light intensity (Figures 4 and 5). To clearly show this dependence, we plotted the kinetic curves in the coordinates:

$$-\ln\frac{\mathrm{Abs}_\infty - \mathrm{Abs}(t)}{\mathrm{Abs}_\infty - \mathrm{Abs}_0} \quad \text{vs} \quad I \times \text{time}$$

Here, Abs(t), Abs_0, and Abs_∞ are the current, initial, and steady-state sample absorbance values, and I is the light intensity. The product of light intensity and time is defined as exposure. In these coordinates, the slope of the kinetic curve for monomolecular photo reaction of equivalent particles is independent of the light intensity.

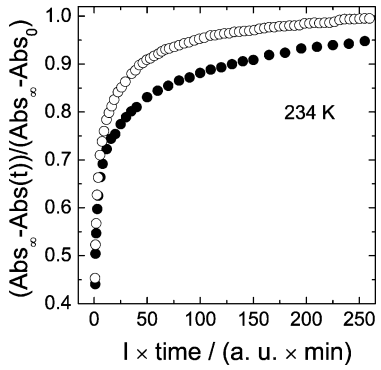

Figure 6. Kinetics of photoisomerization of NAMB in OTP at light intensity 0.533 (solid circles) and 0.126 a.u. (open circles). The initial parts of the curves are not shown.

Figure 4 shows that at 244 K and light intensity of 0.0419 a.u., isomerization kinetics is practically exponential. At lower temperature, the isomerization kinetics does not follow the exponential law at any light intensity used in the present work. In addition, the isomerization kinetics does not follow the exponential law at 244 K and high light intensity (0.236 and 1 au).

It is convenient to introduce the relative rate of absorbance change per unity of light flux:

$$k(t) = \frac{1}{\mathrm{I}(\mathrm{Abs}_\infty - \mathrm{Abs}(t))}\frac{\mathrm{dAbs}(t)}{\mathrm{d}t} \qquad (2)$$

This value sets the slope of curves in Figures 4 and 5.

Figure 6 depicts the dependence of the absorbance on the exposure for two light intensities, 0.126 and 0.533 au. The figure clearly demonstrates that at small exposure values, a change in absorbance per one photon is larger in the case of low light intensity. At high exposure values, the situation is the inverse. The depicted kinetic curves cannot be brought into coincidence either by selecting the Abs_∞ value or by changing the time scale for one of the curves. Therefore, we conclude that the dependence of the $k(t)$ value on the light intensity is not the artifact caused by inaccurate determination of the Abs_∞ value.

Figure 4c shows the kinetic curve for photoisomerization of NAMB under noncontinuous irradiation with a light of intensity 1 au (crosses). The irradiation periods of τ were followed by dark periods of 3τ. As a result, the average intensity of the light was 1/4 au. One can see that the kinetics is the same as in the case of continuous irradiation with a light of intensity 0.236 a.u. (open circles). This fact supports the idea that the change in the value of $k(t)$ with varying light intensity is due to some dark processes only.

3.2. Why Does the Change of Absorbance per Photon Depend on Light Intensity? Probable Reasons. The obtained set of data testifies unambiguously to the existence of dark processes leading to the restoration of an initial particle distribution over the reactivity. There are two kinds of the processes; namely, (1) the rotation of probe molecules and (2) the dynamics of their local environment. Let us consider them in turn.

The rotation of particles leads to the restoration of initial distribution if the latter is caused only by the different orientations of the transition dipoles of molecules with respect to the light polarization vector. In our experiments, the molecules whose transition dipoles are transverse to a light beam absorb light (and react) with the greatest probability. The molecules whose transition dipoles is directed along the beam absorb light

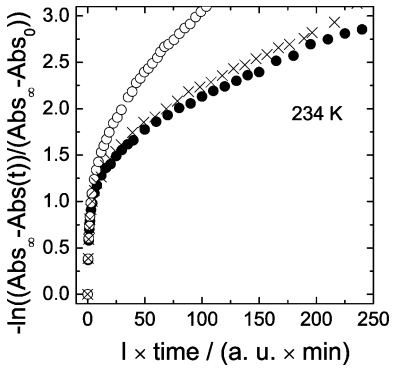

Figure 7. First-order plots for photoisomerization of NAMB in OTP. Solid circles, irradiation with light of intensity 0.533 a.u. along one direction; open circles, irradiation with light of intensity 0.126 a.u. along one direction; crosses, isotropic irradiation with light of intensity 0.523 a.u.

with a probability equal to zero. Therefore, in the case of rotation, the effective rate constant will be higher when the sample is irradiated with light of a lower intensity.

To verify this hypothesis, we have carried out a special experiment under conditions of isotropic irradiation of the sample that exclude the "orientational" kinetic nonequivalence of dye molecules. To simulate isotropic irradiation, the sample (the plastic ampule was used) was irradiated alternately along the X and Y axes during equal periods. The XYZ system is rigidly bound to the sample, as shown in Figure 1. To irradiate the sample along the Y axis, we turned it around the Z axis through 90°.

The sample was irradiated along the X axis through the set of neutral glasses (NS6 and BS15, transmittance at 546 nm is 0.695) and along Y through the polarizer (transmittance at 546 nm for unpolarized light is 0.351). The polarizer was used to get a horizontally polarized light. If the time periods are short, this irradiation procedure is equivalent to the simultaneous irradiations along axes *x, y,* and *z* with light of identical intensity. Under these conditions, the mean effective light intensity is equal to $(0.695 + 0.351)/2 = 0.523$ a.u.

The kinetics obtained under the "isotropic" irradiation was compared with that obtained under irradiation along the X axis. To obtain the "one-direction" kinetics, we irradiated the sample along X with unpolarized light through the set of neutral glasses NS1, BS3, BS8 (total transmittance at 546 nm is 0.533). The value of filter transmittance was chosen to provide the same total photon flux in the "isotropic" and "one-direction" irradiation methods. Actually, the difference in the photon fluxes did not exceed 2%.

Figure 7 demonstrates that the kinetic curves for the cases of "isotropic" and "one-direction" irradiation differ very negligibly. For comparison, the figure also shows the kinetic curve for the case of sample irradiation in one direction with light of low intensity (the intensity being 0.126 a.u.). One can see, that effective rate constant is essentially higher in the case of sample irradiation with light of low intensity. We conclude, then, that an increase in isomerization efficiency with decreasing light intensity is due to the change in the local environment of a molecule.

3.3. Model. Under conditions of dynamical heterogeneity, the monomolecular reaction can be generally described in terms of a distribution function over rate constants, $C(k, t)$, and a probability function, $W(k, t; k_1, t + dt)$, which determines the probability that at time $t + dt$ the particle will have the rate constant k_1 if at t it had the rate constant k. We assume that the function $W(k, t; k_1, t + dt)$ is time-independent. Therefore, we can write $W(k, t; k_1, t + dt) = W(k; k_1)$. Thus, we assume that the relaxation of matrix, as a whole, is missing in the course of the reaction.

To describe the kinetics of isomerization, we used a simplified distribution; namely, a trimodal one. It was assumed that each particle belongs to one of three ensembles whose weights $C_i(t)$ are determined by matrix properties. Fitting showed that this distribution describes well the experimental kinetic curves.

Under conditions of dynamical heterogeneity, the trimodal distribution is characterized by six transitions probabilities (or exchange constants), W_{ij} for the transitions of molecules from the *i*th ensemble to the *j*th. We assume that the initial distribution is equilibrium. Then, taking into account the principle of detailed balance,

$$\frac{W_{ij}}{W_{ji}} = \frac{C_j(0)}{C_i(0)} \tag{3}$$

we reduce the number of independent W_{ij} values to three. Here, $C_i(0)$ are the weights of the ensembles prior to reaction.

In addition, we assume that the probability of transition from ensemble k to ensemble i is proportional to the weight of the *i*th ensemble, which can be written as the following:

$$\frac{W_{ki}}{W_{kj}} = \frac{C_i(0)}{C_j(0)} \tag{4}$$

The set of eqs 3 and 4 reduces the number of independent values W_{ij} to one, in terms of which the rest can be given.

On irradiation with 546 nm light, the steady-state fraction of the trans isomer is five times as high as that of the cis isomer. Therefore, in our simulations, we neglected the trans → cis process. As a result, the set of kinetic equations describing the cis → trans isomerization is of the form

$$\frac{dC_i(t)}{dt} = -k_i C_i(t) - \sum_{j \neq i} W_{ij} C_i(t) + \sum_{j \neq i} W_{ji} C_j(t) \tag{5}$$

3.4. Calculation Procedure and Results. To solve eq 5, one need know the effective rate constants, k_i. These values were determined from the kinetic curves recorded at high light intensity ($I = 1$). At $I = 1$, the exchange time much exceeds the characteristic time of isomerization (by an order of magnitude in the range 204−239 K and by a factor of 3 at 244 K). Therefore, at high light intensity, we neglected the exchange processes and considered that the local environments do not change during the isomerization. The isomerization kinetics were described by the sum of exponential processes, and the k_i values were determined by fitting the kinetic curves with the sum of three exponents.

In the second stage, we determined the exchange rate constants using kinetic curves at low light intensity. The W_{ij} values were found from the numerical solution of eq 5, which provided the best coincidence between the calculated and experimental kinetic curves. Figure 5 depicts the typical calculated kinetic curves.

The ensemble average exchange time is determined using the following equation:

$$\tau_{ex} = \sum_i \frac{C_i(0)}{\sum_{j \neq i} W_{ij}} \tag{6}$$

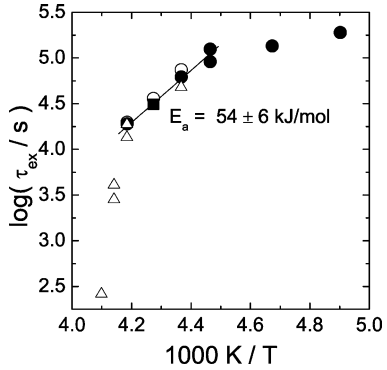

Figure 8. Arrhenius plot for the exchange time. The exchange times were extracted from the kinetic curves obtained at light intensities of 0.236 and 1 au (solid circles), 0.0419 and 1 au (open circles), 0.126 and 0.533 au (square) using the plastic ampule and light intensities of 0.236 and 1 au using the Pyrex ampule (triangles). The solid line is the result of fitting of all the data in the range 224−239 K using the Arrhenius equation.

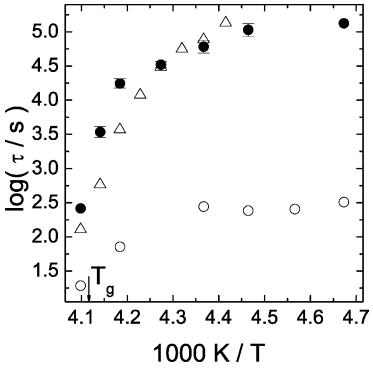

Figure 9. Arrhenius plots for the characteristic times of different processes: exchange process (solid circles), rotation (triangles), and cis−trans isomerization at $I = 1$ (open circles). The exchange times are average values obtained using the data shown in Figure 8; the error bars are one standard deviation. The rotation times are taken from ref 38. The parameter τ_{KWW} of KWW fitting function is taken as the isomerization time.

Figure 8 shows the Arrhenius plot for the τ_{ex} value. One can see that the data obtained using various ampules and different light intensities are in fair agreement. The activation energy of τ_{ex} is determined to be 54 ± 6 kJ/mol over the range of 224−239 K. As the temperature drops below 224 K, the increase in exchange time slows down.

The τ_{ex} value measured at 244 K is 260 s, which differs from the value for 239 K ($\sim 1.7 \times 10^4$ s) by almost 2 orders of magnitude. We can conclude, then, that the strongest decrease in exchange rate occurs near T_g.

3.5. Comparison with Literature Data. A characteristic time of OTP α-relaxation at 244 K estimated from ref 39 is ∼100 s, which is almost three times as small as the exchange time measured in the present work (260 s). The β-relaxation is characterized by a value that is several orders of magnitude shorter than the exchange time.[39,40]

In ref 19, the method of single molecule spectroscopy was used to measure the lifetime of the environment of the rhodamine 6G molecule in OTP at temperatures slightly exceeding T_g. A value of $\sim 1.1 \times 10^3$ s was obtained at 245 K. The lifetime of the environment was determined as the mean time during which the rotation rate of the molecule is constant.

Ediger and co-workers[14,15] have measured the time of structural OTP relaxation over the range of 244−247 K. The structural relaxation time was defined as the time necessary for restoring the initial distribution of tetracene molecules by rotation times upon destruction of the most rapid particles (60% of the total number) under the intense light pulse. According to the data at 244 K, the time of the restoration of initial distribution amounts to $\sim 10^5$ s.

The exchange time obtained in the present work at 244 K is close to the value measured in ref 19 at 245 K. Taking into account a weak temperature dependence of the exchange time determined in 19, this value should not change much as the temperature decreases by 1 K.

The difference in the data of Ediger and co-workers[15] and the data presented in this work is large enough. This may be caused by use of different values as a criterion of exchange. In ref 15, the value of the structural relaxation time was defined as the time necessary for full restoration of the initial distribution over tetracene rotation times. In the present work and in ref 19, the lifetime of the local environment of a probe molecule was measured. This time can differ from the time of initial distribution restoration measured in ref 15 due to the different probability of various transformations of the local environment.

In the case of isomerization, the complete restoration of the molecule distribution by reactivity upon photolysis with light of very low intensity should lead to exponential kinetics. However, only the kinetics obtained at 244 K and light intensity of 0.0419 a.u. is close to exponential. Taking into account the fact that the restoration of the molecule distribution by reactivity can exhibit the nonexponential, strongly prolonged character, the total time required for restoring the initial distribution can substantially exceed the values obtained in the present work. Remember that in the model proposed, all processes are considered exponential. In the real matrix, the transitions of a molecule from the *i*th ensemble to the *j*th can correspond to the range of exchange rates.

Figure 9 shows the temperature dependence for different processes involving the molecules of NAMB; namely, the exchange, the cis−trans isomerization, and the rotation.[38] The isomerization time is defined as parameter τ_{KWW} of the Kohlrausch−Williams−Watts (KWW) function used to approximate the kinetics of isomerization. We can distinguish two different temperature regions: a region higher than ≃234 K and a region below ≃234 K. At temperatures higher than 234 K, the rotation time is less than the obtained exchange time (note that authors of works 15 and 19 also found that the rotation time of probe molecules is less than the exchange time). For example, in the range 239−241.5 K, the ratio τ_{ex}/τ_{rot} is ∼5. In contrast to that, at temperatures below 234 K, the obtained values of the exchange time virtually coincide with the rotation times.

This coincidence is most likely due to the method of exchange time estimation used in the present work. The simple model used here suggests that the exchange rate is the same for all the molecules that belong to the same ensemble. This is probaably not true, and a wide range of exchange rates can be attributed to each ensemble. Under conditions of heterogeneity, only the molecules having an exchange rate that exceeds the rate of isomerization (when the low light intensity is used) provide an increase in the quantum yield of isomerization. The exchange rates for other molecules can be much less. Thereby, the obtained exchange rate is overestimated and, therefore, can be used as the upper bound. At the same time, the exchange times obtained using light intensities of 0.0419 and 0.236 (at 229, 234, and 239 K; see Figure 8) are in close agreement. This fact bears out that the overestimation is not too large.

Under conditions of heterogeneity, the higher the ratio τ_{ex}/τ_r is, the higher the overestimation of the exchange rate is. We

think that this is the reason why the exchange time coincides with the rotation time at temperatures below 234 K.

The exchange process and the rotation weakly depend on temperature below 234 K. The characteristic time of cis−trans isomerization in this region practically does not depend on temperature. Such behavior of three different processes probably points to weak change in structural and dynamical properties of the matrix below 234 K. Due to a low rate of structural relaxation, the matrix structure in the region below 234 K is similar to the structure at 234 K. The matrix structure is not in equilibrium in this region. This out-of-equilibrium state can be characterized by means of an additional parameter named as fictive temperature.[41,42]

4. Conclusions

A new method, based on the measurement of the photoisomerization kinetics of probe molecules, is proposed to monitor dynamical heterogeneity in glassy matrixes at temperatures below T_g. The method has been used to measure the characteristic times required for the local environment to change over the temperature range of 204−244 K in glassy OTP. An increase in the exchange time with decreasing temperature is strong near T_g and slows down at temperatures much below T_g. The activation energy of structural relaxation is estimated to be 54 kJ/mol over the range of 224−239 K.

Acknowledgment. This work was partially supported by the funds of interdisciplinary integration project of the Siberian Branch of the Russian Academy of Science No. 50.

References and Notes

(1) Angell, C. A.; Ngai, K. L.; McKenna, G. B.; McMillan, P. F.; Martin, S. W. *J. Appl. Phys.* **2000**, *88*, 3113.
(2) Ediger, M. D. *Annu. Rev. Phys. Chem.* **2000**, *51*, 99.
(3) Sillescu, H. *J. Non-Cryst. Solids* **1999**, *243*, 81.
(4) Sillescu, H. *J. Phys.: Condens. Matter* **1999**, *11*, A271.
(5) Bohmer, R.; Hinze, G.; Jorg, T.; Qi, F.; Sillescu, H. *J. Phys.: Condens. Matter* **2000**, *12*, A383.
(6) Diezemann, G.; Bohmer, R.; Hinze, G.; Sillescu, H. *J. Non-Cryst. Solids* **1998**, *235−237*, 121.
(7) Sillescu, H.; Bohmer, R.; Diezemann, G.; Hinze, G. *J. Non-Cryst. Solids* **2002**, *307−310*, 16.
(8) Richert, R. *Europhys. Lett.* **2001**, *54*, 767.
(9) Jeffrey, K. R.; Richert, R.; Duvvuri, K. *J. Chem. Phys.* **2003**, *119*, 6150.
(10) Huang, W.; Richert, R. *J. Chem. Phys.* **2006**, *124*, 164510.
(11) Russell, E. V.; Israeloff, N. E. *Nature* **2000**, *408*, 695.
(12) Patkowski, A.; Fischer, E. W.; Steffen, W.; Glaser, H.; Baumann, M.; Ruths, T.; Meier, G. *Phys. Rev. E: Stat. Phys., Plasmas, Fluids, Relat. Interdiscip. Top.* **2001**, *63*, 061503.
(13) Patkowski, A.; Glaser, H.; Kanaya, T.; Fischer, E. W. *Phys. Rev. E: Stat. Phys., Plasmas, Fluids, Relat. Interdiscip. Top.* **2001**, *64*, 031503.
(14) Cicerone, M. T.; Ediger, M. D. *J. Chem. Phys.* **1995**, *103*, 5684.
(15) Wang, C.-Y.; Ediger, M. D. *J. Phys. Chem. B* **1999**, *103*, 4177.
(16) Wang, C.-Y.; Ediger, M. D. *J. Chem. Phys.* **2000**, *112*, 6933.
(17) Yang, M.; Richert, R. *Chem. Phys.* **2002**, *284*, 103.
(18) Wang, L.-M.; Richert, R. *J. Chem. Phys.* **2004**, *120*, 11082.
(19) Deschenes, L. A.; Vanden Bout, D. A. *J. Phys. Chem. B* **2002**, *106*, 11438.
(20) Schob, A.; Cichos, F.; Schuster, J.; von Borczyskowski, C. *Eur. Polym. J.* **2004**, *40*, 1019.
(21) Vallee, R. A. L.; Cotlet, M.; Hofkens, J.; De Schryver, F. C.; Mullen, K. *Macromolecules* **2003**, *36*, 7752.
(22) Tolkatchev, V. A. Kinetics of the Simplest Radical Reactions in Solids. In *Reactivity of Solids: Past, Present and Future*; Boldyrev, V. V., Ed.; JUPAC, A Chemistry for 21st Century; Blackwell Science: Oxford, 1996; p 185.
(23) Eisenbach, C. D. *Polym. Bull.* **1980**, *2*, 169.
(24) Richert, R. *Macromolecules* **1988**, *21*, 923.
(25) Imamura, Y.; Yamaguchi, Y.; Tran-Cong, Q. *J. Polym. Science B: Polym. Phys.* **2000**, *38*, 682.
(26) Ilieva, D.; Nedelchev, L.; Petrova, Ts.; Dragostinova, V.; Todorov, T.; Nikolova, L.; Ramanujam, P. S. *J. Opt. A: Pure Appl. Opt.* **2006**, *8*, 221.
(27) Victor, J. G.; Torkelson, J. M. *Macromolecules* **1987**, *20*, 2241.
(28) Yu, W.-C.; Sung, C. S. P.; Robertson, R. E. *Macromolecules* **1988**, *21*, 355.
(29) Mita, I.; Horie, K.; Hirao, K. *Macromolecules* **1989**, *22*, 558.
(30) Anseth, K. S.; Rothenberg, M. D.; Bowman, C. N. *Macromolecules* **1994**, *27*, 2890.
(31) Janus, K.; Matczyszyn, K.; Sworakowski, J. *Mater. Sci.* **2002**, *20*, 45.
(32) Park, J.-W.; Ediger, M. D.; Green, M. M. *J. Am. Chem. Soc.* **2001**, *123*, 49.
(33) Richert, R. *Chem. Phys.* **1988**, *122*, 455.
(34) Richert, R.; Heuer, A. *Macromolecules* **1997**, *30*, 4038.
(35) Zimmerman, G.; Chow, L.; Paik, U. *J. Am. Chem. Soc.* **1958**, *80*, 3528.
(36) Greet, R. J.; Turnbull, D. *J. Chem. Phys.* **1967**, *46*, 1243.
(37) Becker, H.; Berger, W.; Domschke, G.; Fanghanel, E.; Faust, J.; Fischer, M.; Gentz, F.; Gewald, K.; Gluch, R.; Mayer, R.; Muller, K.; Pavel, D.; Schmidt, H.; Schollberg, K.; Schwetlick, K.; Seiler, E.; Zeppenfeld, G. *Organicum*, 15th ed.; VEB Deutscher Verlag der Wissenschaften: Berlin, 1976.
(38) Grebenkin, S. Yu.; Bol'shakov, B. V. *J. Phys. Chem. B* **2006**, *110*, 8582.
(39) Wagner, H.; Richert, R. *J. Phys. Chem. B* **1999**, *103*, 4071.
(40) Johari, G. P.; Goldstein, M. *J. Chem. Phys.* **1970**, *53*, 2372.
(41) Tool, A. Q.; Eichlin, C. G. *J. Am. Ceram. Soc.* **1931**, *14*, 276.
(42) Alegria, A.; Guerrica-Echevarria, E.; Telleria, I.; Colmenero, J. *Phys. Rev. B: Condens. Matter Mater. Phys.* **1993**, *47*, 14857.